THE JOURNAL OF PHYSICAL CHEMISTRY B
A JOURNAL OF THE AMERICAN CHEMICAL SOCIETY

pubs.acs.org/JPCB

Article

Field-Driven Reversible Alignment and Gelation of Magneto-Responsive Soft Anisotropic Microbeads

Published as part of The Journal of Physical Chemistry virtual special issue "Carol K. Hall Festschrift".

Natasha I. Castellanos, Bhuvnesh Bharti, and Orlin D. Velev*

Cite This: *J. Phys. Chem. B* 2021, 125, 7900–7910

Read Online

ACCESS | Metrics & More | Article Recommendations | Supporting Information

ABSTRACT: Magnetic fields offer untethered control over the assembly, dynamics, and reconfiguration of colloidal particles. However, synthesizing "soft" colloidal particles with switchable magnetic dipole moment remains a challenge, primarily due to strong coupling of the dipoles of the adjacent nanoparticles. In this article, we present a way to overcome this fundamental challenge based on a strategy to synthesize soft microbeads with tunable residual dipole moment. The microbeads are composed of a polydimethylsiloxane (PDMS) matrix with internally embedded magnetic nanoparticles (MNPs). The distribution and orientation of the MNPs within the PDMS bead matrix is controlled by an external magnetic field during the synthesis process, thus allowing for the preparation of anisotropic PDMS microbeads with internal magnetically aligned nanoparticle chains. We study and present the differences in magnetic interactions between microbeads containing magnetically aligned MNPs and microbeads with randomly distributed MNPs. The interparticle interactions in a suspension of microbeads with embedded aligned MNP chains result in the spontaneous formation of percolated networks due to residual magnetization. We proved the tunability of the structure by applying magnetization, demagnetization, and remagnetization cycles that evoke formation, breakup, and reformation of 2D percolated networks. The mechanical response of the microbead suspension was quantified by oscillatory rheology and correlated to the propensity for network formation by the magnetic microbeads. We also experimentally correlated the 2D alignment of the microbeads to the direction of earth's magnetic field. Overall, the results prove that the soft magnetic microbeads enable a rich variety of structures and can serve as an experimental toolbox for modeling interactions in dipolar systems leading to various percolated networks, novel magneto-rheological materials, and smart gels.

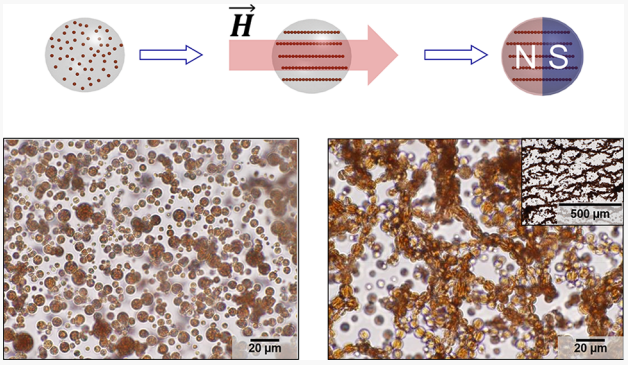

INTRODUCTION

The ability to provide a structural response to environmental conditions is embedded in the genetic makeup of many living beings.[1−3] Enabling such response in synthetic colloidal matter holds the key to encode life-like features in future generations of artificial materials.[2,4−7] One example of a natural response to external fields is found in magnetotactic bacteria.[1] These bacteria synthesize iron oxide nanoparticles within their cytoplasm and create a permanent magnetic dipole that enables the bacteria to sense the surrounding magnetic field and to reconfigure and coordinate their movement. They can thus swim along the direction of earth's magnetic field while seeking to find optimal conditions for their survival.[6] The chain(s) of magnetic nanoparticles internalized in the bacteria act as a means of navigation to find favorable habitats.[8] An ability to incorporate micro- and nanosized particles within beads mimicking magnetotactic orientation could provide new means for designing magneto-responsive materials, which reconfigure in response to external environments and stimuli.

Colloidal particles which change their physical and/or chemical state in response to external stimuli such as temperature,[9] electrical and magnetic fields,[10] and pH[7,11] can find numerous applications such as targeted drug delivery,[6] biomolecular separations, smart structures, and soft actuators.[12−14] One such class of responsive materials are magnetic colloids, which alter their assembled state in response to the presence of external magnetic field.[15−18] Magnetic colloids dispersed in aqueous or nonaqueous medium, commonly known as ferrofluids, interact via magnetic forces in addition to conventional colloidal forces such as van der Waals and electrostatics.[19−21] Programming these interactions and direct-

Received: April 8, 2021
Revised: June 14, 2021
Published: July 13, 2021

ing the morphology of colloidal assemblies coupled in space and time is one the strategies of encoding nonequilibrium response in artificial matter. The assembly and reconfiguration of magnetic colloids is governed by the physical state of the constituting particles, which could be ferromagnetic, ferrimagnetic, or superparamagnetic.[21,22]

Ferromagnetic materials refer to the class of magnetic materials which can retain their magnetic moment even after the external field is removed. These ferromagnetic materials have permanent dipole moment and behave as microscale magnets.[6] One problem that is often encountered with such particles in a dispersing medium is the lack of colloidal stability, i.e., the ferromagnetic particles are prone to spontaneous aggregation. The sum of van der Waals and magnetic dipolar forces exceeds the ability of Brownian motion to disrupt the strongly attractive structure.[23] To prevent this aggregation, it is necessary either to introduce a repulsive force barrier between the particles by adding surface adsorbed amphiphiles[24] or immobilizing the nanoparticles inside a larger matrix. In this article, we find a way to use the latter strategy and investigate the impact of spatial distribution of magnetic nanoparticles (MNPs) within an elastomer matrix of carrier microbeads on their magnetic response.

Magnetorheological elastomers,[21,25] magneto-colloidal fluids,[16,26,27] gels,[3,28−30] and foams[31−33] comprise classes of smart materials whose rheological properties can be controlled by an external magnetic field.[8] There is also large effort toward the formation of responsive soft materials with internal magnetic anisotropy, whose macroscopic response is guided by particle structures assembled within the soft composites. Such structures can be fabricated by the assembly of particles inside a polymerizable medium and later cross-linking of the polymer matrix, so the positions of the particles remain fixed within the embedding polymer network.[34−36] Thus, the structural motif remains embedded after the external magnetic field applied during the synthesis step is removed.[25]

Under uniform magnetic fields or field gradients, the moments of the MNPs align, and the attractive magnetic dipolar forces pull them together, favoring magnetization along the direction of the field and leading to chaining.[6,37−41] These chainlike assemblies or percolated networks can, depending on the packing fraction of the sample of microbeads, span the whole sample because of the magnetically induced particle chaining within the matrix.[5] The magnetic and mechanical properties of such long-ranged assembles can be strongly coupled to make magnetically controlled matrices where nano- or micrometer-sized magnetic particles have been embedded in the elastomers.[42,43] The MNPs within the soft composites can be either distributed randomly or organized in chains.[30,34,43] The MNPs used in such responsive composites are usually made of iron oxides (such as γ-Fe_2O_3 and Fe_3O_4),[16,39,44] metals or alloys (containing metals such as Fe, Co, Ni, Fe, and Pt), or iron nitride particles which can also be biologically compatible. Furthermore, in the absence of an external field, chainlike structures can form loops or arrangements that can lead to the formation of the gel phase.[25] Synthesizing such composite colloidal particles with tunable magnetic properties remains a challenge and is a key focus of this study.

We present here the design, synthesis, and characterization of a class of soft microbeads (SMBs) made of an elastomeric matrix containing either randomly distributed or aligned chains of MNPs. The suspensions of magneto-responsive soft particles are made by a scalable technique that enabled us to synthesize polydimethylsiloxane (PDMS) microbeads with embedded MNPs. The resulting SMBs show a number of distinctly different assembly modes, and rheological responses in the presence and absence of external magnetic field. We describe how these soft microbeads exhibit responsive, switchable, and reversible binding driven by magnetic interactions. We demonstrate and analyze their orientation, assembly, and disassembly in the presence of magnetizing and demagnetizing fields.

MATERIALS AND METHODS

Dispersing MNPs within the PDMS Precursor Medium. Depending on the desired weight percent of MNPs in the final PDMS microbead suspension, 2.5, 5, or 10 wt % iron(III) oxide nanoparticles (20 nm, MKNano) were added to 36 g of tetrahydrofuran (THF) in a round-bottomed flask and sonicated for 1 h. THF was added to temporarily reduce the viscosity of the PDMS precursor (Sylgard 184 obtained from Dow) such that the particles could be uniformly dispersed in the silicone emulsion. The required amount of PDMS prepolymer was then added to the round-bottomed flask, and the mixture was further sonicated for 5 h to ensure uniform distribution of particles in the solvent. The THF was then evaporated from the mixture, leaving the PDMS precursor with internalized MNPs.

Synthesis of PDMS Microbeads Containing Randomly Distributed MNPs. PDMS is a cross-linkable polymer with a Young's modulus tunable by the molar ratio of PDMS base and the cross-linker. The synthesis of microbeads from PDMS includes emulsification and cross-linking of PDMS by precursor and curing agent. First, a 14 wt % poly(vinyl alcohol) (PVA) solution was made by heating and stirring for 2 h a mixture of 100 g of deionized (DI) water (18.2 MΩ cm at 25 °C, obtained from a Millipore Milli-Q Academic water purification system) at 120 °C, to which we added 16.28 g of poly(vinyl alcohol) (PVA) (Mowiol 18−88, Sigma-Aldrich) in a covered beaker. The exact weight percent of the PVA in solution was determined gravimetrically. The PVA−water solution (40 mL) was then placed in a beaker and mixed at 150 rpm in a mechanical mixer with an impeller, while the PDMS was mixed and degassed. The addition of the PVA was necessary because of the large mismatch of the high viscosity of PDMS (3500 cP) and the low viscosity of water (1 cP), which produces very polydisperse PDMS droplets during shearing of the dispersion. The addition of the PVA to the water phase allowed the formation of much more uniform droplets.[45] The 10:1 mixture of PDMS/cross-linker Sylgard 184 was then injected into the 14% PVA solution while it was being mixed, and the suspension was stirred at 150 rpm for 10 min to ensure homogenization. The emulsion was then refined further by mixing at 250 rpm for an hour. Once the mixing was complete, the emulsion was placed in an oven at 60 °C overnight to accelerate the cross-linking process of the polymer matrix. The PDMS microbeads were then washed several times with an aqueous solution of Tween 20 (0.1 wt %) using a vortex mixer and a centrifuge. Determination of the final weight percent of the PDMS SMB dispersion was done gravimetrically, and in this report, our chosen final weight percent was 50 wt % magnetic PDMS microbeads in aqueous solution of 0.1 wt % Tween 20.

Synthesis of PDMS Microbeads Containing Magnetically Aligned MNPs. These microbeads were made by a process similar to the PDMS microbeads with randomly distributed embedded MNPs. The main difference was that an external magnetic field (19 mT) was applied parallel to the chamber walls during the whole overnight curing period. This

https://doi.org/10.1021/acs.jpcb.1c03158
J. Phys. Chem. B 2021, 125, 7900−7910

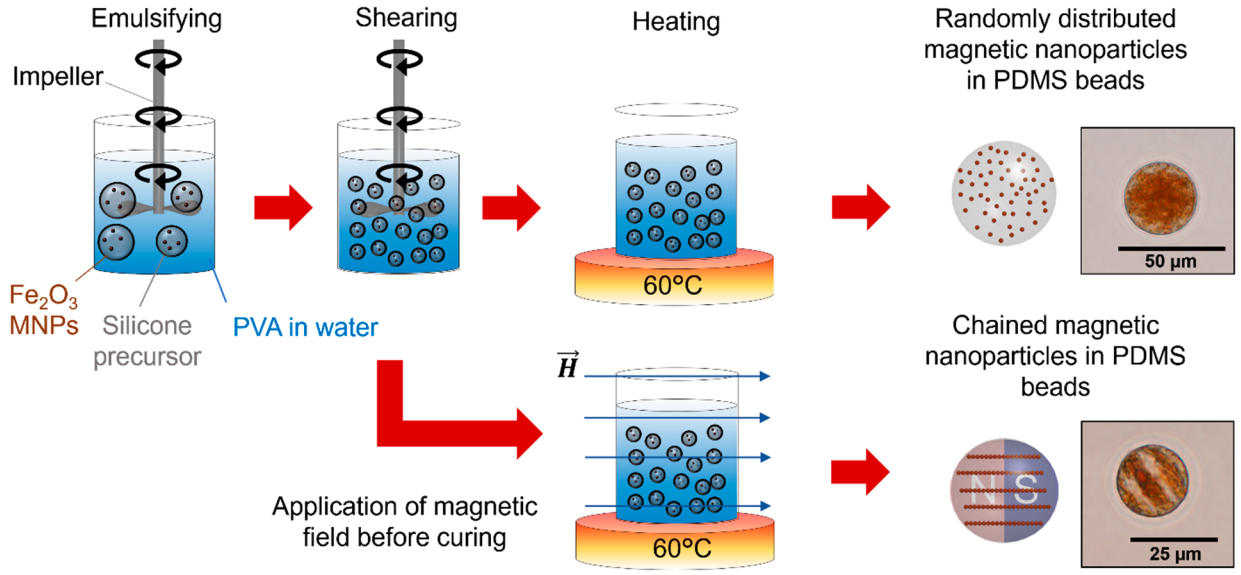

Figure 1. Schematics of the method of synthesizing PDMS microbeads with embedded iron(III) oxide nanoparticles using an emulsification technique. The internal organization of the magnetic nanoparticles can be preserved if the soft microbeads (SMBs) are cured under a magnetic field. The SMB microscope image examples shown are bigger than those typically used for the experiments (10 μm) for better visualization.

resulted in the formation of PDMS microbeads with locked-in dispersion or magnetically aligned chains of the MNPs embedded in the silicone matrix (Figures 1, S1, and S2). A table-top demagnetizer was used to demagnetize the beads.

Rheological Analysis of Magnetic Microbead Suspensions. Rheological analysis of the suspensions was performed using a DHR-2 rheometer (TA Instruments , New Castle, DE) with serrated parallel plate geometry (diameter = 40 mm with 0.5 mm gap size). Sandpaper was used to minimize the effect of wall slip during the experiments. Angular frequency sweeps were conducted at 1% strain for 100−0.03 rad s^{-1}. The amplitude oscillatory measurements were conducted within the linear viscoelastic regime of the samples. The linear viscoelastic regime was determined by performing oscillatory strain sweeps at a constant angular frequency of 10 rad sec^{-1}. The samples were covered with a homemade solvent trap to prevent water evaporation. All tests were performed at a constant temperature of 25 °C.

Optical Microscopy and Cell Orientation. Optical microscopy (Olympus, BX-61) with an Olympus DP-70 digital CCD camera was used to characterize the morphology of the magnetic PDMS microbeads. Magnetization and demagnetization studies were also conducted and recorded with the chained microbeads suspension. The orientation of earth's magnetic field in the location of the experimental chamber and throughout the laboratory were determined by a hand-held iPhone 11 compass sensor.

Magnetometry. The magnetization of the MNP-containing gels was characterized using the Quantum Design MPMS 3 SQUID/VSM magnetometer. The device was calibrated using a reference sample made of Pd. The samples were run in direct current (dc) mode at room temperature and at atmospheric pressure.

RESULTS AND DISCUSSION

The microbead emulsion fabrication process, regardless of the application or not of external magnetic field, resulted in spherical PDMS microbeads with an average diameter of 10 μm (Figure 2). The individual magnetic particles inside these microbeads could not be resolved in the microscopy images due to their small size. However, after the external magnetic field is applied during the synthesis (Figure 2a), magnetically aligned particle chains can be clearly observed as lines embedded in the PDMS microbeads (Figure 2c, S1b, and S2) as opposed to scattered or randomly distributed particle clusters in the microbead (Figure 2b and S1a). After the magnetic field is turned off, these two types of SMB suspensions interact and assemble to form drastically different patterns, as seen in the microscopy images in Figure 2b,c. Although the concentration of both types of magnetic PDMS microbeads is high and attractive interactions between microbeads in both cases can be observed to lead to some clustering, the SMBs with randomly distributed MNPs remains generally dispersed in suspension and not interconnected on a longer scale (Figure 2b). The SMB suspensions with embedded aligned MNPs, however, display the formation of percolated or branched networks (Figure 2c).

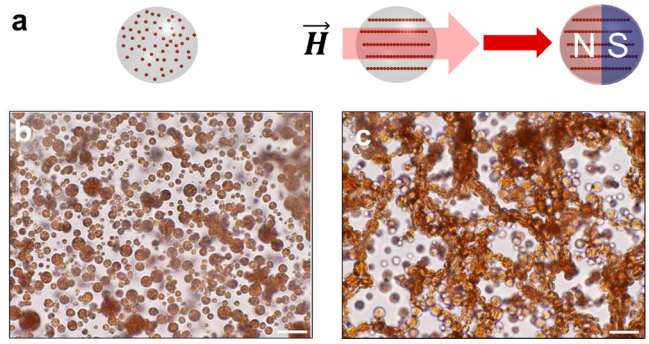

Figure 2. (a) Magnetic elastomer spheres dispersed in water where the embedded MNPs can have two different orientations by having either (b) embedded randomly distributed iron(III) oxide nanoparticles (10 wt %, no field applied) or (c) magnetically aligned iron(III) oxide nanoparticles (10 wt %, field of 19 mT applied during curing). Scale bars are 20 μm.

https://doi.org/10.1021/acs.jpcb.1c03158
J. Phys. Chem. B 2021, 125, 7900−7910

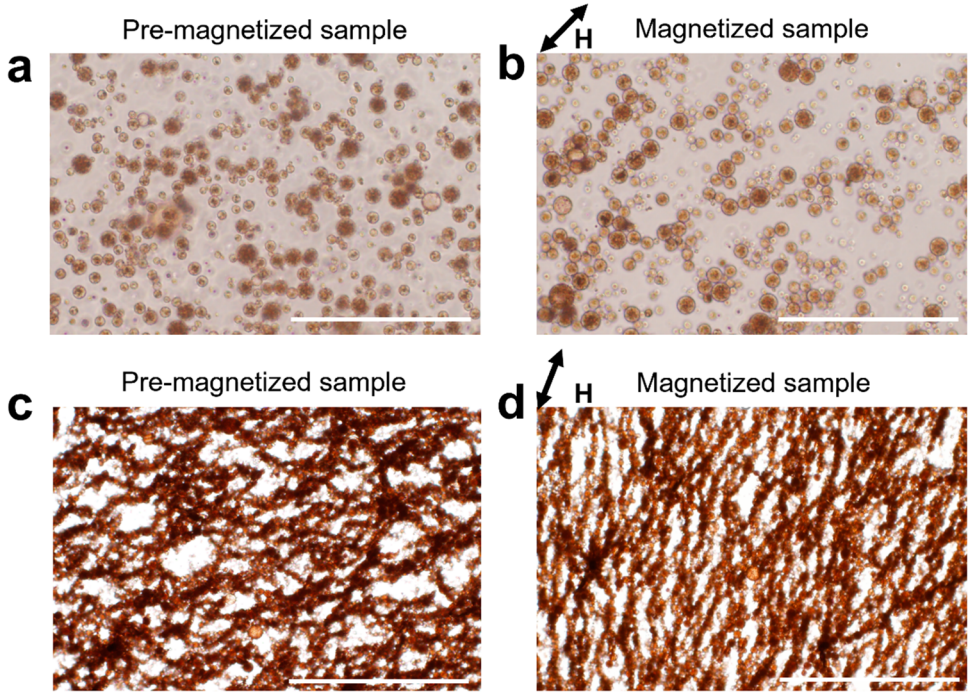

Figure 3. Magnetic interactions in SMB suspensions (50 wt % PDMS microbeads in water, each containing 10 wt % MNPs) can vary. (a) When MNPs are randomly dispersed inside, the microbeads do not appear to interact without the presence of an external magnetic field even when they have been subjected to external field earlier ("pre-magnetized"). (b) They demonstrate very weak chaining and branching only if the system is subjected to a magnetic field (19 mT). (c) Microbeads with embedded magnetically aligned MNPs form branched networks when premagnetized, even if an external field is not applied, and (d) they form organized percolated networks and align in the direction of an applied magnetic field (19 mT). Scale bars are 200 μm.

This structure formation was investigated further by subjecting each microbead type to a permanent external magnetic field of 19 mT. The SMBs with randomly distributed MNPs showed little to no interaction before the application of the external field (Figure 3a). Once a field was applied, these microbeads became partially structured in as little as 15 s, forming a few short linear chains and bundles (Figure 3b). However, these structures were not uniform in the bulk suspension, and they easily and almost immediately broke apart if the suspension was mechanically disturbed or if the magnetic field was removed. The SMBs containing aligned MNPs clearly formed long-range linear flexible branched structures even when no additional external field was applied while in suspension (Figure 3c). This is a result of their remanent magnetization (premagnetization) during the application of the external field during the fabrication process. Once an external field was applied to the SMBs with aligned MNP chains, these initially randomly branched structures rapidly reoriented and reorganized in the direction of the field in as little as 3 s (Figure 3d). Moreover, after being formed and magnetized with an external field (19 mT) the structures almost immediately ($\approx$ 1 s) reassembled if the system was disturbed, indicating that the microbeads with aligned MNPs had residual polar magnetization or magnetic memory. The fascinating dynamics of self-reassembly of such premagnetized SMBs is illustrated in Movie S1.

The assembly of microbeads with nonaligned MNPs in an external field is driven by the polarization of the nanoparticles within the SMB PDMS matrix. In the presence of external field, the magnetic domains within the embedded MNPs endow the SMBs with a net magnetic dipole moment. This induced dipole leads to the formation of well-known bead chain necklace type assembly of the SMBs. The assembled SMB structures with randomly internalized MNPs break up upon switching off the external magnetic field. The observed SMB disassembly agrees with a previous study on the assembly/disassembly of superparamagnetic microspheres in response to field on and off cycles.[2] The previously reported disassembly was attributed to the rapid decrease/disappearance of magnetic moment of the microparticles upon switching off the external magnetic field. In our case of microbeads with nonaligned MNPs, the origin of the observed disassembly is similarly a result of decrease in magnetic attraction upon switching off the external field, combined with the surface charge repulsions and hydrodynamic interactions.

In contrast, the SMB structures with prealigned chains do not disassemble upon switching off the external magnetic field but reconfigured to form a percolated network. The lack of disassembly is due to the magnetic retentivity of the microbeads with aligned chains, where the residual magnetization allows them to more readily interact with neighboring microbeads, leading to rapid percolation. Once magnetized, the SMB system with aligned MNP chains formed percolated networks even without the presence of an external field (Figure 3c). This local residual magnetization and corresponding structural relaxation into a percolated network of microbeads imparts specific viscoelastic and self-reassembly characteristics of the microbead suspension (discussed later). The formation of percolated networks in such types of interacting dipolar systems has been predicted and modeled theoretically previously.[5,46−51] It can be noted that at high concentrations the spontaneous chaining in systems without applied field is not in any specific direction and displays branching, often at the junction of one large and two smaller beads. Once we applied a magnetic field, however, the branched SMB network became much more uniformly aligned

https://doi.org/10.1021/acs.jpcb.1c03158
J. Phys. Chem. B 2021, 125, 7900−7910

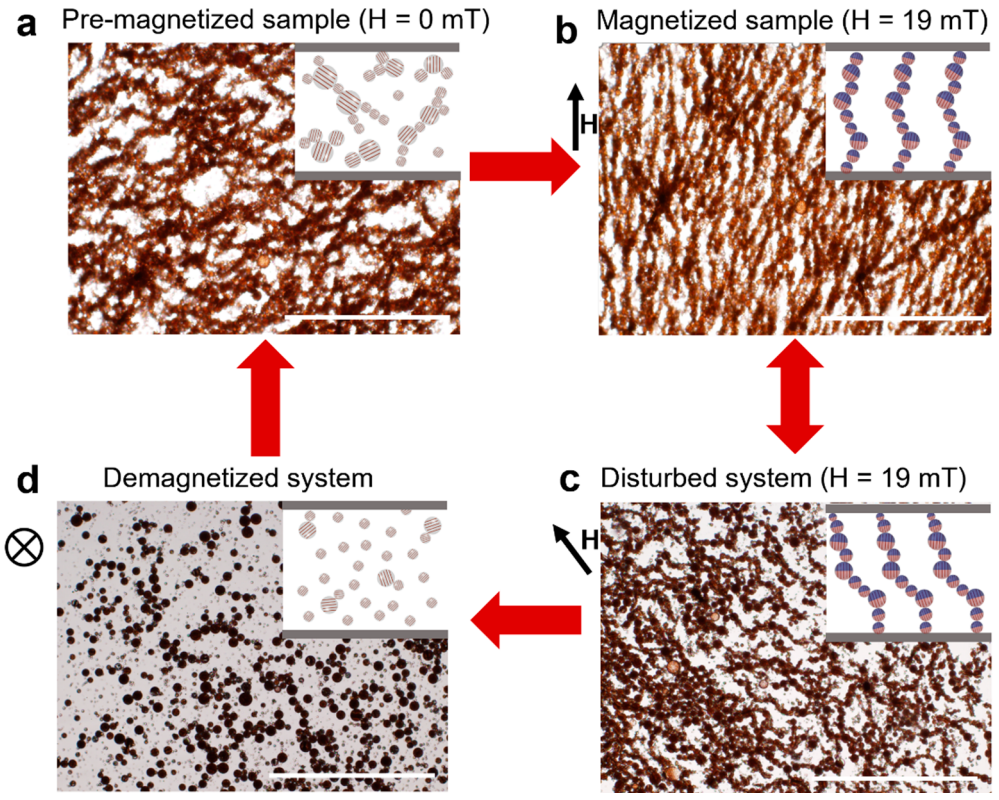

Figure 4. Magnetically aligned microbead system demonstrated tunability by using reversible magnetization. (a) Aligned PDMS microbeads form branched networks even if no external magnetic field is applied due to the premagnetization during fabrication and (b) form more organized branched structures when an external field is applied (H = 19 mT). (c) These long-ranged structures break apart when the system is disturbed but can reform almost immediately. (d) They can break down into mostly individual microbeads if the suspension is demagnetized but can reassemble when remagnetized. The black arrows indicate the direction of the external magnetic field. Scale bars are 200 μm.

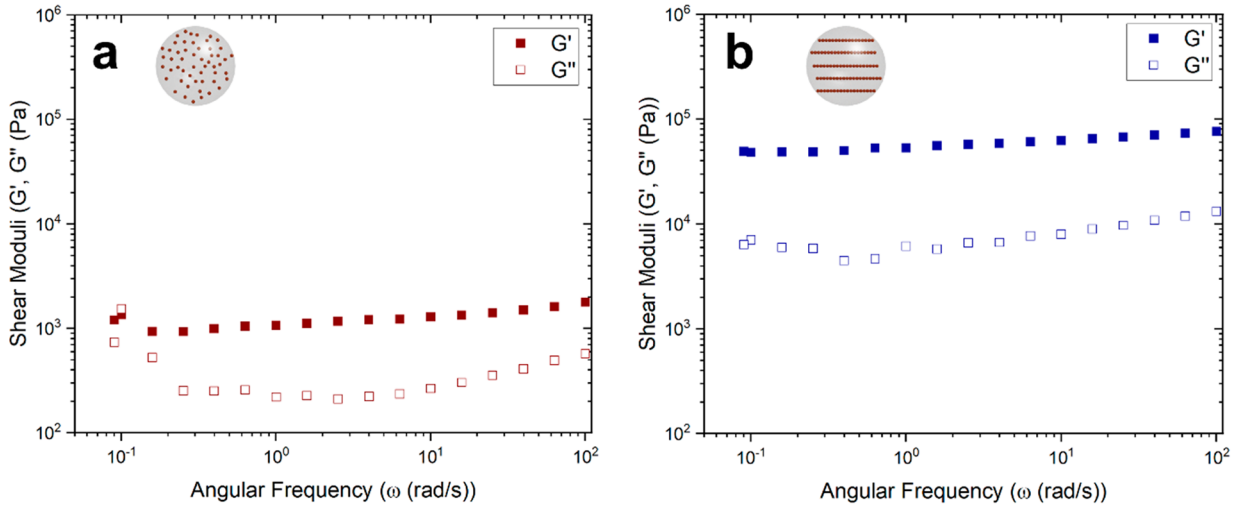

Figure 5. Storage, G', and loss, G'', moduli as a function of frequency for each type of magnetic microbead. (a) The lack of interactions between the SMBs with randomly distributed MNPs demonstrates lower G' and G'' and more liquidlike properties, whereas (b) the weak interactions between the magnetically aligned SMBS with embedded chains lead to magnetic force-induced structuring or a "soft" gel-like properties (50 wt % PDMS microbead to water, 10 wt % embedded MNPs).

and structured, with chaining in the applied field direction (Figure 3d). The long-range permanently assembled structure of extended and in occasionally branched chains formed by the microbeads can be realigned by an application of fields in different directions (shown in Movie S2).

The percolated structures from internally aligned magnetic particles do not experience spontaneous disassembly over time as the particles can sustain their dipolar polarization. Even if such a network is strongly disturbed by stirring or other mechanical disturbance, it reforms. However, there is a simple and efficient technology solution for resetting this system to its original dispersed, weakly interacting state. Soft magnets can be demagnetized by applying an alternating magnetic field of decaying intensity through a demagnetizer coil operated by a

https://doi.org/10.1021/acs.jpcb.1c03158
J. Phys. Chem. B 2021, 125, 7900−7910

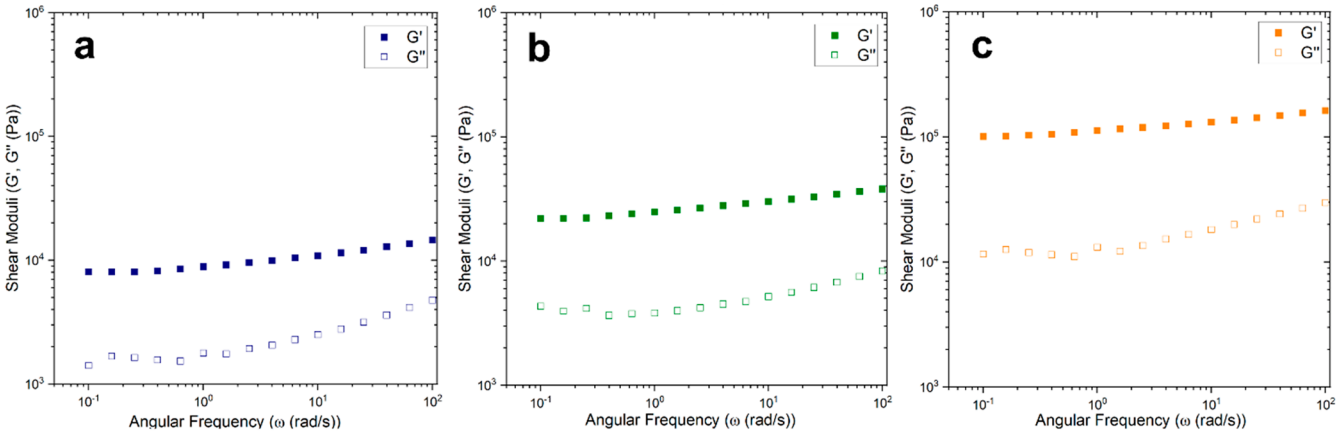

Figure 6. Storage, G', and loss, G'', moduli as a function of frequency for magnetic microbeads with (a) 2.5 wt %, (b) 5 wt %, and (c) 10 wt % aligned MNPs embedded in the SMB PDMS matrix. The gel strength increases as the number of MNPs loaded in the microbeads increases.

corresponding circuit.[52] During this process, the ferromagnetic domains within the nanoparticles are "forced" to reorient multiple times, while their moment is reduced in a preprogrammed way. This technique was used by us previously for triggered disassembly of magnetic Janus particles.[53] The use of the technique is illustrated in Figure 4. When the suspension of magnetically aligned PDMS microbeads (Figure 4a–c) was subjected to a demagnetizing field, it experienced a large reduction of the residual magnetization. The change is evident in the microscopy image in Figure 4d and in the dynamics of the particles in Movie S3, where the initial chain-like structure was disassembled in the demagnetizer field, and a suspension of discrete, spatially separated microbeads was obtained. The magnetic moment of the microbeads can be regained by remagnetization, and a percolated structure of microbeads can be reassembled to return to the initial state of the SMBs as shown in Figure 4a. Thus, we have a two-state switchable system, with long-range structuring capabilities.

Rheology of Both Types of Magnetic SMBs. The observed formation of large-scale percolated structures indicates the possible occurrence of phenomena such as gelation in macroscopic bulk systems. The formation of percolated and entangled particle networks is a common prerequisite for gelation.[5,51,54] The occurrence of gelation can be confirmed by macroscopic change in a few physical properties.[55] One common mechanical technique for characterizing the onset of gelation is rheology.[56] The magnetic alignment of the microbeads should affect their gelation; moreover, it will be dependent on the type of particles present in the system. We investigated the rheological response of SMB systems with both nonaligned and aligned MNPs, subjected to small amplitude oscillatory shear experiments aimed to be within the linear viscoelastic regime of the suspensions. Their storage (G') and loss (G'') moduli were measured as a function of the angular frequency (ω).

A comparison of the rheological response of the two types of microbead samples is presented in Figure 5. The sample of microbeads with randomly distributed MNPs appeared to be in a transition state, suggesting a very weak gel-like structuration, because G' is of the same magnitude and almost equal to G'' at lower frequencies (Figure 5a). The sample of SMBs with magnetically aligned MNPs demonstrated gel-like behavior with $G' \gg G''$ at 50 wt % PDMS microbeads to water in the entire range of frequency sweep (Figure 5b). These data suggest that the beads with aligned particles formed magnetic-induced gels with a strong tolerance to external deformations/perturbations since it maintained its gel-like state throughout the whole frequency range (Figure 5). This sample has G' of approximately one order of magnitude higher than G'' and hence tan (δ) of less than 1. The moduli of the microbead sample with aligned MNPs were several orders of magnitude greater than those of the sample with microbeads with randomly distributed nanoparticles, suggesting that the gel strength of the chained microbead sample is greater. This observation is further evidenced by the G' and G'' of regular, nonmagnetic microbeads. These beads had a G' and G'' several orders of magnitude smaller than that of either type of magnetic microbeads (actual G'= 2.734 Pa and G''= 1.944 Pa at 1 rad/s). This result indicates that the long-chain organization of the soft magnetic particles containing MNP chains with residual polarization assists with the formation of robust, magnetically actuatable gels. However, these gels differ from common molecular gels in that they do not show any stretchability (due to which the Young's modulus could not be measured).

The rheology experiments also made it possible to determine the correlation between the fraction of magnetic material loaded into the SMBs and gel stiffness. The properties of SMB gels with increasing concentrations of magnetic particles embedded in the PDMS bead matrix (2.5, 5, and 10 wt %) were characterized, while preserving the overall SMB concentration at 50 wt % with respect to the aqueous Tween 20 (Figure 6). That is, all three bead types had the same constant 50 wt % SMB concentration and varied only by the amount of MNPs embedded in the beads. By comparing the frequency sweep of each concentration of magnetic nanoparticles, we observed an increase in moduli with the microbead concentration. This is expected as an increase in the volume fraction of the MNPs will increase the attractive interactions and the gel strength of the magnetically aligned microbead system. This trend was also observed in the randomly distributed MNPs microbead system (data not shown), which suggests that this trend is independent of the orientation of the MNPs. We hypothesize that this increase is a result of the increasing magnetic attraction when more magnetic material is embedded in the microbeads leading to magnetically induced gel strength. One simple, albeit semiquantitative, way of checking this hypothesis is to normalize the shear moduli by the weight percent of the MNPs that are used to lace them. For example, in the case of the microbeads with 2.5 wt % MNPs, the

https://doi.org/10.1021/acs.jpcb.1c03158
J. Phys. Chem. B 2021, 125, 7900−7910

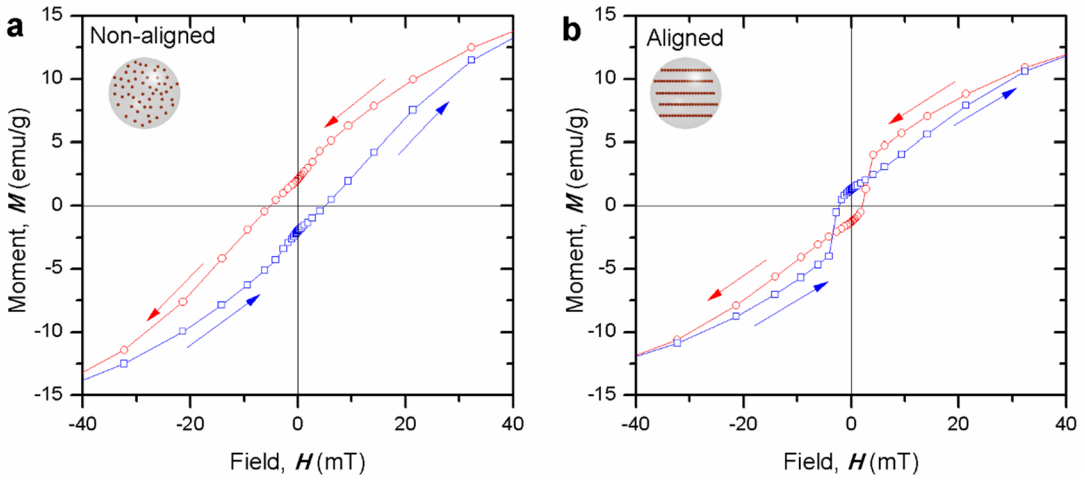

Figure 7. Magnetization curves for (a) microbeads with randomly distributed MNPs and (b) microbeads with embedded, magnetically aligned MNPs. These curves represent the normalized magnetic moment of the beads containing 10 wt % of MNPs as a function of the applied magnetic field. The arrows indicate the scan direction, when the applied field goes up or down during the measurement.

overall weight of the MNPs in the gel was 1.25 wt % since the beads were 50 wt % in suspension. The curves for all normalized shear and loss moduli are plotted in Figure S3. As seen, renormalizing the rheology data resulted in good (but not complete) clustering of the curves highlighting a heuristic correlation between the weight percent of MNPs in the microbeads and the viscoelasticity of the dispersion. This allows to design simple rules for gel formulation. Further interpretation of the magnetic gelation data required measurement of the magnetic polarizability of the soft microbead system, which is described in the next section.

Magnetometry Characterization of the Microbeads. The data for particle structuring and gelation indicate the key role of the particle polarizability and remanent magnetic polarization in governing the viscoelastic properties of the suspensions. In order to evaluate these effects, the magnetic properties of the particle suspensions were investigated with a SQUID magnetometer. The samples were measured in unidirectional magnetic field (±2 T) at room temperature and atmospheric pressure in a water/glycerol liquid mixture to reduce sedimentation during the experiment. The magnetization curve is determined by measuring the change in the net moment of the suspension upon increasing and decreasing external magnetic field cycles.

The magnetization curves for microbeads containing 10 wt % MNPs in the nonaligned configuration show hysteresis which is characteristic of ferromagnetic material (Figure 7a). The residual moment of a microbead can be evaluated from these data by $\boldsymbol{\mu}_r = M\,(\text{at } \boldsymbol{H} = 0) \times m$, where $\boldsymbol{M}$ (at $\boldsymbol{H} = 0$) is the residual magnetic moment and m is the mass of MNPs within a microbead. We estimate that the residual moment in each microbead with nonaligned MNPs is $\boldsymbol{\mu}_r \sim 3.3 \times 10^{-14}$ Am^2. The determination of magnetic moment of a bead with aligned chains is nontrivial due to an anomaly in the magnetometry (discussed below). By assuming a linear decrease of the moment in the demagnetizing field in the region $\boldsymbol{H} < 20$ mT, we estimate a retentivity by extrapolating magnetometry data to $\boldsymbol{H} = 0$ mT. We find that the residual magnetic moment of a bead with aligned nanoparticle chains (10 wt %) is $\boldsymbol{\mu}_r \sim 1.8 \times 10^{-13}$ Am^2. Here we use point−dipole approximation to estimate the interparticle interaction between two SMBs (of diameters = 10 μm). According to point-dipole approximation, the interaction energy (U_{mag}) between two dipoles i and j is given as[S7]

$$U_{mag} = \frac{1}{\mathbf{r}_{ij}^3}\left[\mu_i \cdot \mu_j - 3\frac{(\mu \cdot \mathbf{r}_{ij})(\mu_j \cdot \mathbf{r}_{ij})}{\mathbf{r}_{ij}^2}\right]$$

where $\boldsymbol{\mu}$ is the dipole moment and $\mathbf{r}_{ij}$ is the position vector joining the centers of the interacting particles. We recognize that the point−dipole approximation only provides a crude estimation of the interaction energy, and the effects of mutual polarization and multibody interactions of the beads should be taken into account for a precise determination of the energy, especially at short separations.[58−60] Here we use the point−dipole model to provide a qualitative relationship between the interaction energy among beads with aligned and nonaligned MNPs, and a more comprehensive analysis would be necessary for obtaining absolute magnetic energy of the ensemble, which is beyond the scope of present experimental study.

The calculated interaction energy as a function of the separation between two identical microbeads of diameter 10 μm with nonaligned and aligned MNPs is plotted in Figure 8. We find that the interaction energy between the microbeads at surface contact is significantly higher than the thermal energy (i.e., kT, k being the Boltzmann constant and T the temperature), but it rapidly decreases upon increasing the interparticle separation. The larger moment of the beads with aligned MNPs in comparison to beads with nonaligned MNPs results in a much stronger interaction which leads to the persistence of the chained network-like structure of beads with aligned MNPs even upon turning off the magnetic field (Figures 3 and 8). However, the interaction energy calculations based on magnetometry data suggest that the microbeads with nonaligned MNPs would retain their assembled structure, as interaction energy exceeds thermal fluctuations, which is not observed in the experiments (Figure 3). This discrepancy points to the role of nonmagnetic repulsive interactions such as electrical double-layer repulsions and localized hydrodynamic interactions in the microbead suspensions,[2] which lead to disruptive energies larger that simple thermal diffusion. Further work on mathematical modeling of such interactions would be necessary to fully understand the unusual experimental behavior of the microbeads.

https://doi.org/10.1021/acs.jpcb.1c03158
J. Phys. Chem. B 2021, 125, 7900−7910

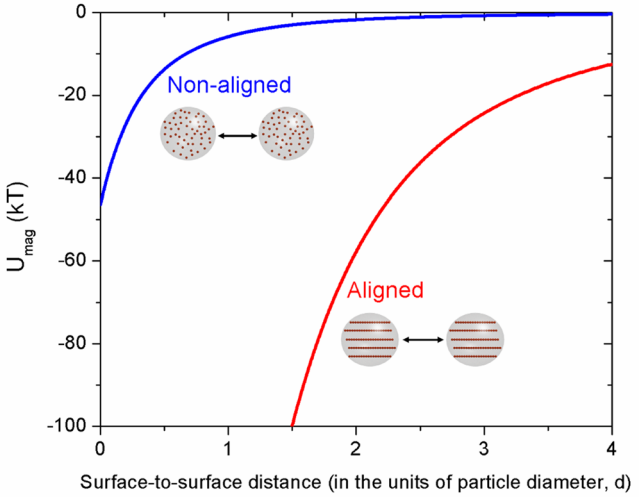

Figure 8. Estimated interaction energy between two PDMS microbeads with 10 wt % nonaligned and aligned MNPs embedded in the PDMS matrix (d = 10 μm).

The microbeads with aligned MNPs show a peculiar split hysteresis loop (Figure 7). This unusual loop is a signature of dynamical changes occurring in the liquid suspension during the magnetization and demagnetization cycles. It is notable that no such split hysteresis has been reported previously for colloidal dispersions and that the origin of this behavior has not been reported. The alignment of the MNP chains within the PDMS matrix render the particle magnetically anisotropic. We believe that following two factors may contribute to split hysteresis: (a) free rotation and reorientation of the microbeads in the suspension upon decreasing the field from the magnetic saturation (at ∼100 mT) and (b) reversal of magnetization via domain wall movement. In our case, the magnetometry was performed in liquid suspensions where the particles are free to reorient. Here, upon decreasing the magnetic field from its saturation point, the particles may reorient while partially preserving their magnetic moment, thus leading to the observed split hysteresis where at a low field of ∼10 mT an inversion of the magnetic polarity is observed. Additionally, it has been shown that for magnetically anisotropic films the split hysteretic loop exists due to the reversal of magnetization at the edges of the film due to domain wall movement upon decreasing the field.[61−63] In our case, the SMBs possess magnetic anisotropy. Due to the presence of aligned MNPs in the SMBs, the edges of the particles may show a reversal of magnetization in demagnetizing field and such effect dominates near the switching fields (i.e., −10 to +10 mT). We recognize that based on our experiments it is not feasible to predict the relative contributions of the two factors mentioned above leading to the observed split hysteretic behavior of microbeads with aligned MNPs chains. Further experimental and theoretical investigations are necessary to interpret the unusual observed magnetic behavior of our colloidal SMBs in magnetization−demagnetization−remagnetization cycles.

Long-Range Organization of the Microbeads in Weak Magnetic Fields. One of the intriguing behaviors observed with the PDMS beads with aligned particle chains is the long-distance alignment of both the particle chains and the MNP chains inside them in the same angular direction. This phenomenon, which is observed in dilute systems with distinct individual microbead chains is illustrated by the micrograph in Figure 9. We hypothesized that the alignment is caused by earth's magnetic field, similar to the orientation of compass needles. To check that prediction, a compass was used to determine the direction of earth's magnetic field, and it was confirmed that the microbeads align co-linearly with earth's magnetic north−south axis.

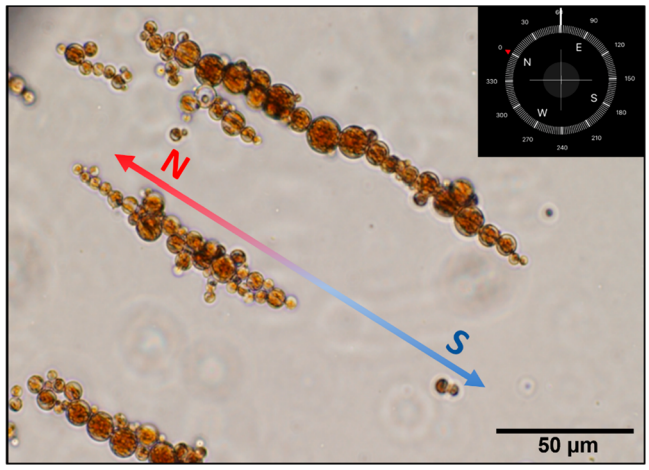

Figure 9. Magnetic microbeads orient and organize in ways so that the embedded magnetic particle chains face the same direction and form linear structures that align in the direction of earth's magnetic field (sample is 10 wt % MNPs in SMBs, the direction of the earth' field is shown in the compass sensor image). Such an orientation presents a fascinating analogy with the one observed with magnetotactic bacteria in nature.

The origin of this alignment requires theoretical evaluation, as the beads and even their assemblies are orders of magnitude smaller than the typical compass magnet. Thus, we evaluated the energy of orientation of the beads in earth's magnetic field. The energy of a magnetic dipole ($\boldsymbol{\mu}$) in a uniform magnetic field ($\boldsymbol{B}$) is given as $U_d(\theta) = -\boldsymbol{\mu}\cdot\boldsymbol{B} = -\mu B \cos\theta$, where θ is the angle between the dipole moment vector and the direction of the magnetic field.[64] Therefore, the change in energy upon rotating a dipole from orientation θ_1 to θ_2 is estimated as $\Delta U_d = -\mu B(\cos\theta_2 - \cos\theta_1)$. The origin of the reorientation of a dipole in the external field is the lowering of configuration energy given by ΔU_d. Here we assume that $\Delta U_d = kT$ (i.e., at least 1 kT energy is required to reorient the dipole). The minimum dipole moment of such a particle which will reorient from 45 to 0° in earth's magnetic field (∼4 × 10^{-5} T) is ∼3.5 × 10^{-16} A m^2, which is about one-hundreth of the dipole moment of our microbeads (see the previous section). Therefore, in dilute systems where the microbeads could rotate freely, they would align along the magnetic north−south axis.

The phenomenon of long-range arrangement has a fascinating biomimetic analogy. As mentioned in the introduction, a broadly similar phenomenon of MNPs chains orientation in living matter is observed in the alignment of magnetotactic bacteria in earth's magnetic field. The SMBs' response to earth's magnetic field due to their residual magnetic polarization could also influence the physical understanding and interpretation of the structure formation in such systems. The modeling of dipolar particles structuring to date assumes a system with random initial dipolar orientation.[5,18] The imposition of earth's or other weak fields could affect both the directionality and length scale of the resulting percolated structures. At this stage, it is not immediately clear whether the alignment of the individual

https://doi.org/10.1021/acs.jpcb.1c03158
J. Phys. Chem. B 2021, 125, 7900−7910

SMB chains along earth's magnetic field, observed in the thin chamber, would affect the properties and behavior of the dense 3D SMB systems such as the gels described in the previous section. While this effect is much weaker than the electromagnetic actuation in the experimental cell, the structural impact of the beads' prealignment by the earth's field, or other weak fields, warrants further theoretical and experimental investigation.

CONCLUDING REMARKS

This study was made possible by the introduction of a class of SMBs that combines two useful features of their constituent materials: the use of matrix of common PDMS elastomer and the magnetic responsivity of the embedded MNPs. Notably, the synthesis of these soft beads by an emulsification procedure is nontrivial in addressing the need to produce droplets of uniform size and a relatively narrow size distribution in this size range. We produced relatively uniform droplets by shearing of the liquid silicone precursor in a PVA solution with matching viscosity.[45] The elastomer microbeads were proven to be a colloidal system that is easy to make and scale up to macroscopic quantities, while the internal structure of the MNPs in the SMBs could be controlled by external field.

These magnetic microbeads can serve as an experimental toolbox for modeling interactions in dipolar systems, leading to various percolated networks, novel magneto-rheological materials, and smart gels. The formation of percolated networks in similar types of interacting dipolar systems has been predicted and modeled theoretically by Hall and collaborators.[46−50,54] We showed that the interactions and structure formation of the SMB systems could be drastically changed by aligning the embedded magnetic nanoparticles. We proved through microscopy that the microbeads formed different percolated networks structures depending on the magnetic alignment of the MNPs. It was demonstrated that an external magnetic field could direct the assembly of the system and that the aligned microbeads reassembled into long-ranged chains after dispersion. We showed that these SMBs with aligned MNPs have residual polar magnetization and gel-like properties. We proved the tunability of this system by conducting magnetization, demagnetization, and remagnetization experiments that were evidence of the reformation of percolating networks.

The use of these beads as model systems in understanding and controlling magnetic interactions could in the future be enhanced in a variety of ways. First, further improvements of the particle synthesis procedures could enable more precise control and uniformity of the MNP chains in the SMB matrix (including making SMBs with a single coaxial MNP chain). It might be possible to deploy microfluidics in order to increase monodispersity in the SMBs size, if desired, or even to be able to visualize the individual MNPs embedded in the SMBs as done by Chen et al.[65] The chain structure and distribution in the SMBs can be visualized by using 3D electron tomography. Second, a better understanding of the fundamentals of two-body and multibody interactions could be of benefit for modeling and control. Two-bead interactions could be measured by methods such as analysis of distribution of distances between particles or by capturing beads with optical tweezers and AFM. Finally, prealignment with weak fields could be used to improve the connectivity and other structural aspects of the final soft gel materials.

These beads can also be used in several applied areas. The transparent beads with aligned chains can serve as convenient microprobes in visualizing even very weak magnetic fields on the microscale. Such particles can also be used in biomedical applications, as particles that can be magnetically moved and guided are promising in applications such as drug delivery and cancer therapies.[66,67] Our microbeads with aligned MNPs have the potential to be used as vehicles for applications such as targeted delivery, as they can be easily loaded with molecular "cargo" and their alignment and location can be precisely controlled by an external magnetic field. Finally, as the method is easily scalable, these classes of elastomeric magnetic beads can find applications in larger-scale "smart" stimuli-responsive materials with switchable phase transitions.

ASSOCIATED CONTENT

Supporting Information

The Supporting Information is available free of charge at https://pubs.acs.org/doi/10.1021/acs.jpcb.1c03158.

High-magnification optical microscopy images of silicone microbeads with nonaligned and aligned MNPs and a combined plot of the magnetic gel normalized storage, G', and loss, G'', moduli as a function of frequency for magnetic microbeads (PDF)

Movie S1: SMBs with magnetically aligned MNPs being disrupted and gradually reassembling into long-range percolated network in the absence of external field. Movie is sped up 2×. (MP4)

Movie S2: SMBs with magnetically aligned MNPs form percolated networks having the ability to reform after they are magnetized (19 mT) and disturbed. Scale bar is 200 μm. (MP4)

Movie S3: Demagnetized SMBs with magnetically aligned MNPs demonstrate little to no interactions due to the removal of the permanent magnetization. Scale bar is 200 μm. (MP4)

AUTHOR INFORMATION

Corresponding Author

Orlin D. Velev − *Department of Chemical and Biomolecular Engineering, North Carolina State University, Raleigh, North Carolina 27695, United States;* orcid.org/0000-0003-0473-8056; Email: odvelev@ncsu.edu

Authors

Natasha I. Castellanos − *Department of Chemical and Biomolecular Engineering, North Carolina State University, Raleigh, North Carolina 27695, United States*

Bhuvnesh Bharti − *Cain Department of Chemical Engineering, Louisiana State University, Baton Rouge, Louisiana 70803, United States;* orcid.org/0000-0001-9426-9606

Complete contact information is available at: https://pubs.acs.org/10.1021/acs.jpcb.1c03158

Notes

The authors declare no competing financial interest.

ACKNOWLEDGMENTS

The authors express gratitude to Professor Carol K. Hall for numerous research collaborations, collegial interactions, inspiration, and leadership. N.I.C. and O.D.V. acknowledge financial support from the National Science Foundation (NSF) awards CBET-1604116 and CBET-1935248. The contributions to the manuscript by B.B. were supported by NSF award CBET-

2038305. We thank Dr. Lilian Hsiao for the use of the rheometer, Dr. Lewis Reynolds for assistance with magnetometry measurements and discussions, and Dr. Joseph Tracy for the valuable discussions on magnetic properties of the MNPs and SMBs.

REFERENCES

(1) Blakemore, R. P. Magnetotactic Bacteria. *Ann. Rev. Microbiol.* **1982**, *36*, 217−238.
(2) Bharti, B.; Velev, O. D. Assembly of Reconfigurable Colloidal Structures by Multidirectional Field-Induced Interactions. *Langmuir* **2015**, *31*, 7897−7908.
(3) Lalitha, K.; Prasad, Y. S.; Sridharan, V.; Maheswari, C. U.; John, G.; Nagarajan, S. A renewable resource-derived thixotropic self-assembled supramolecular gel: magnetic stimuli responsive and real-time self-healing behaviour. *RSC Adv.* **2015**, *5*, 77589−77594.
(4) Ahn, S.-K.; Kasi, R. M.; Kim, S.-C.; Sharma, N.; Zhou, Y. Stimuli-responsive polymer gels. *Soft Matter* **2008**, *4*, 1151−1157.
(5) Goyal, A.; Hall, C. K.; Velev, O. D. Bicontinuous gels formed by self-assembly of dipolar colloid particles. *Soft Matter* **2010**, *6*, 480−484.
(6) Huang, H.-W.; Huang, T.-Y.; Charilaou, M.; Lyttle, S.; Zhang, Q.; Pané, S.; Nelson, B. J. Investigation of Magnetotaxis of Reconfigurable Micro-Origami Swimmers with Competitive and Cooperative Anisotropy. *Adv. Funct. Mater.* **2018**, 1802110.
(7) Prileszky, T. A.; Furst, E. M. Magnetite nanoparticles program the assembly, response, and reconfiguration of structured emulsions. *Soft Matter* **2019**, *15*, 1529−1538.
(8) Erb, R. M.; Martin, J. J.; Soheilian, R.; Pan, C.; Barber, J. R. Actuating Soft Matter with Magnetic Torque. *Adv. Funct. Mater.* **2016**, *26*, 3859−3880.
(9) Hodaei, A.; Akhlaghi, O.; Khani, N.; Aytas, T.; Sezer, D.; Tatli, B.; Menceloglu, Y. Z.; Koc, B.; Akbulut, O. Single Additive Enables 3D Printing of Highly Loaded Iron Oxide Suspensions. *ACS Appl. Mater. Interfaces* **2018**, *10*, 9873−9881.
(10) Tracy, J. B.; Crawford, T. M. Magnetic field-directed self-assembly of magnetic nanoparticles. *MRS Bull.* **2013**, *38*, 915−920.
(11) Ponton, A.; Bee, A.; Talbot, D.; Perzynski. Regeneration of thixotropic gels studied by mechanical spectroscopy: the effecet of pH. *J. Phys.: Condens. Matter* **2005**, *17*, 821−836.
(12) Wang, M.; Yin, Y. Magnetically Responsive Nanostructures with Tunable Optical Properties. *J. Am. Chem. Soc.* **2016**, *138*, 6315−6323.
(13) Zhang, J.; Huang, Q.; Du, J. Recent advances in magnetic hydrogels. *Polym. Int.* **2016**, *65*, 1365−1372.
(14) Suwa, M.; Uotani, A.; Tsukahara, S. Alignment and small oscillation of superparamagnetic iron oxide nanoparticle in liquid under alternating magnetic field. *J. Appl. Phys.* **2019**, *125*, 123901.
(15) Bharti, B.; Fameau, A.-L.; Velev, O. D. Magnetophoretic assembly of flexible nanoparticle/lipid microfilaments. *Faraday Discuss.* **2015**, *181*, 437−448.
(16) Korth, B. D.; Keng, P.; Shim, I.; Bowles, S. E.; Tang, C.; Kowalewski, T.; Nebesny, K. W.; Pyun, J. Polymer-Coated Ferromagnetic Colloids from Well-Defined Macromolecular Surfactants and Assembly into Nanoparticle Chains. *J. Am. Chem. Soc.* **2006**, *128*, 6562−6563.
(17) Schmidle, H.; Jäger, S.; Hall, C. K.; Velev, O. D.; Klapp, S. H. L. Two-dimensional colloidal networks induced by a uni-axial external field. *Soft Matter* **2013**, *9*, 2518−2524.
(18) Schmidle, H.; Hall, C. K.; Velev, O. D.; Klapp, S. H. L. Phase Diagram of two-dimensional systems of dipole-like colloids. *Soft Matter* **2012**, *8*, 1521−1531.
(19) Bharti, B.; Fameau, A.-L.; Rubinstein, M.; Velev, O. D. Nanocapillarity-mediated magnetic assembly of nanoparticles into ultraflexible filaments and reconfigurable networks. *Nat. Mater.* **2015**, *14*, 1104−1109.
(20) Schmauch, M. M.; Mishra, S. R.; Evans, B. A.; Velev, O. D.; Tracy, J. B. Chained Iron Microparticles for Directionally Controlled Actuation of Soft Robots. *ACS Appl. Mater. Interfaces* **2017**, *9*, 11895−11901.
(21) Bharti, B.; Kogler, F.; Hall, C. K.; Klapp, S. H. L.; Velev, O. D. Multidirectional colloidal assembly in concurrent electric and magnetic field. *Soft Matter* **2016**, *12*, 7747−7758.
(22) Spatafora-Salazar, A. S.; Lobmeyer, D. M.; Cunha, L. H. P.; Joshi, K.; Biswal, S. L. Hierarchical assemblies of superparamagnetic colloids in time-varying magnetic fields. *Soft Matter* **2021**, *17*, 1120−1155.
(23) Wang, M.; He, L.; Yin, Y. Magnetic field guided colloidal assembly. *Mater. Today* **2013**, *16* (4), 110−116.
(24) Roh, S.; Velev, O. D. Nanomaterials Fabrication by Interfacial Templating and Capillary Engineering in Multiphasic liquids. *AIChE J.* **2018**, *64*, 3558−3564.
(25) Byrom, J.; Biswal, S. L. Magnetic field directed assembly of two-dimensional fractal colloidal aggregates. *Soft Matter* **2013**, *9*, 9167−9173.
(26) Kim, M. W.; Han, W. J.; Kim, Y. H.; Choi, H. J. Effect of a hard magnetic particle additive on rheological characteristics of micro-spherical carbonyl iron-based magnetorheological fluid. *Colloids Surf., A* **2016**, *506*, 812−820.
(27) Liu, X.; Kent, N.; Ceballos, A.; Streubel, R.; Jiang, Y.; Chai, Y.; Kim, P. Y.; Forth, J.; Hellman, F.; Shi, S.; et al. Reconfigurable ferromagnetic liquid droplets. *Science* **2019**, *365*, 264−267.
(28) Yu, M.; Ju, B.; Fu, J.; Liu, S.; Choi, S.-B. Magnetoresistance Characteristics of Magnetorheological Gel under a Magnetic Field. *Ind. Eng. Chem. Res.* **2014**, *53*, 4704−4710.
(29) Sorokina, O. N.; Kovarski, A. L.; Lagutina, M. A.; Dubrovskii, S. A.; Dzheparov, F. S. Magnetic Nanoparticles Aggregation in Magnetic Gel Studied by Electron Magnetic Resonance (EMR). *Appl. Sci.* **2012**, *2*, 342−350.
(30) Menzel, A. M. Bridging from particle to macroscopic scales in uniaxial magnetic gels. *J. Chem. Phys.* **2014**, *141*, 194907.
(31) Fameau, A. L.; Lam, S.; Velev, O. D. Multi-stimuli responsive foams combining particles and self-assembling fatty acids. *Chem. Sci.* **2013**, *4*, 3874−3881.
(32) Lam, S.; Blanco, E.; Smoukov, S. K.; Velikov, K. P.; Velev, O. D. Magnetically Responsive Pickering Foams. *J. Am. Chem. Soc.* **2011**, *133*, 13856−13859.
(33) Blanco, E.; Lam, S.; Smoukov, S. K.; Velikov, K. P.; Khan, S. A.; Velev, O. D. Stability and Viscoelasticity of Magneto-Pickering Foams. *Langmuir* **2013**, *29*, 10019−10027.
(34) Mishra, S. R.; Dickey, M. D.; Velev, O. D.; Tracy, J. B. Selective and directional actuation of elastomer films using chained magnetic nanoparticles. *Nanoscale* **2016**, *8*, 1309−1313.
(35) Tarama, M.; Cremer, P.; Borin, D. Y.; Odenbach, S.; Löwen, H.; Menzel, A. M. Tunable dynamic response of magnetic gels: Impact of structural properties and magnetic fields. *Phys. Rev.* **2014**, *90*, 042311.
(36) Biswal, S. L.; Gast, A. P. Micromixing with Linked Chains of Paramagnetic Particles. *Anal. Chem.* **2004**, *76*, 6448−6455.
(37) Faraudo, J.; Andreu, J. S.; Calero, C.; Camacho, J. Predicting the Self-Assembly of Superparamagnetic Colloids under Magnetic Fields. *Adv. Funct. Mater.* **2016**, *26*, 3837−3858.
(38) Tokarev, A.; Gu, Y.; Zakharchenko, A.; Trotsenko, O.; Luzinov, I.; Kornev, K. G.; Minko, S. Reconfigurable Anisotropic Coatings via Magnetic Field-Directed Assembly and Translocation of Locking Magnetic Chains. *Adv. Funct. Mater.* **2014**, *24*, 4738−4745.
(39) Tadic, M.; Kralj, S.; Kopanja, L. Synthesis, particle shape characterization, magnetic properties and surface modification of superparamagnetic iron oxide nanochains. *Mater. Charact.* **2019**, *148*, 123−133.
(40) Kralj, S.; Makovec, D. Magnetic Assembly of Superparamagnetic Iron Oxide Nanoparticle Clusters into Nanochains and Nanobundles. *ACS Nano* **2015**, *9* (10), 9700−9707.
(41) Huang, S.; Pessot, G.; Cremer, P.; Weeber, R.; Holm, C.; Nowak, J.; Odenbach, S.; Menzel, A. M.; Auernhammer, G. K. Buckling of paramagnetic chains in soft gels. *Soft Matter* **2016**, *12*, 228−237.
(42) He, L.; Hu, Y.; Han, X.; Lu, Y.; Lu, Z.; Yin, Y. Assembly and Photonic Properties of Superparamagnetic Colloids in Complex Magnetic Fields. *Langmuir* **2011**, *27*, 13444−13450.

https://doi.org/10.1021/acs.jpcb.1c03158
J. Phys. Chem. B 2021, 125, 7900−7910

(43) Zubarev, A. Y.; Chirikov, D. N.; Borin, D. Y.; Stepanov, G. V. Hysteresis of the magnetic properties of soft magnetic gels. *Soft Matter* **2016**, *12*, 6473−6480.
(44) Oh, J. K.; Park, J. M. Iron oxide-based superparamagnetic polymeric nanomaterials: Design, preparation, and biomedical application. *Prog. Polym. Sci.* **2011**, *36*, 168−189.
(45) Roh, S.; Okello, L. B.; Golbasi, N.; Hankwitz, J. P.; Liu, J. A.-C.; Tracy, J. B.; Velev, O. D. 3D-Printed Silicone Soft Architectures with Programmed Magneto-Capillary Reconfiguration. *Adv. Mater. Technol.* **2019**, *4*, 1800528.
(46) Goyal, A.; Hall, C. K.; Velev, O. D. Self-assembly in binary mixtures of dipolar colloids: Molecular dynamics simulations. *J. Chem. Phys.* **2010**, *133*, 064511.
(47) Rutkowski, D. M.; Velev, O. D.; Klapp, S. H. L.; Hall, C. K. Simulation study on the structural properties of colloidal particles with offset dipoles. *Soft Matter* **2017**, *13*, 3134−3146.
(48) Liao, G.-J.; Hall, C. K.; Klapp, S. H. L. Dynamical self-assembly of dipolar active Brownian particles in two dimensions. *Soft Matter* **2020**, *16*, 2208−2223.
(49) Rutkowski, D. M.; Velev, O. D.; Klapp, S. H. L.; Hall, C. K. The effect of charge separation on the phase behavior of dipolar colloidal rods. *Soft Matter* **2016**, *12*, 4932−4943.
(50) Maloney, R. C.; Hall, C. K. Clustering and Phase Separation in Mixtures of Dipolar and Active Particles in an External Field. *Langmuir* **2020**, *36*, 6378−6387.
(51) Kogler, F.; Velev, O. D.; Hall, C. K.; Klapp, S. H. L. Generic model for tunable colloidal aggregation in multidirectional fields. *Soft Matter* **2015**, *11*, 7356−7366.
(52) Baynes, T. M.; Russell, G. J.; Bailey, A. Comparison of Stepwise Demagnetization Techniques. *IEEE Trans. Magn.* **2002**, *38* (4), 1753−1758.
(53) Smoukov, S. K.; Gangwal, S.; Marquez, M.; Velev, O. D. Reconfigurable responsive structures assembled from magnetic Janus particles. *Soft Matter* **2009**, *5*, 1285−1292.
(54) Goyal, A.; Hall, C. K.; Velev, O. D. Phase diagram for stimulus-responsive materials containing dipolar colloidal particles. *Phys. Rev. E* **2008**, *77*, 031401.
(55) Winter, H. H.; Chambon, F. Analysis of Linear Viscoelasticity of a Crosslinking Polymer at the Gel Point. *J. Rheol.* **1986**, *30* (2), 367−382.
(56) Barrera, C.; Florián-Algarin, V.; Acevedo, A.; Rinaldi, C. Monitoring gelation using magnetic nanoparticles. *Soft Matter* **2010**, *6*, 3662−3668.
(57) Al Harraq, A.; Lee, J. G.; Bharti, B. Magnetic field−driven assembly and reconfiguration of multicomponent supraparticles. *Sci. Adv.* **2020**, *6*, eaba5337.
(58) Komarov, K. A.; Kryuchkov, N. P.; Yurchenko, S. O. Tunable interactions between particles in conically rotating electric fields. *Soft Matter* **2018**, *14*, 9657−9674.
(59) Komarov, K. A.; Yurchenko, S. O. Colloids in rotating electric and magnetic fields: designing tunable interactions with spatial field hodographs. *Soft Matter* **2020**, *16*, 8155−8168.
(60) Komarov, K. A.; Yarkov, A. V.; Yurchenko, S. O. Diagrammatic method for tunable interactions in colloidal suspensions in rotating electric or magnetic fields. *J. Chem. Phys.* **2019**, *151*, 244103.
(61) Oepen, H. P.; Millev, Y. T.; Ding, H. F.; Pütter, S.; Kirschner, J. Field-driven reorientation in ultrathin ferromagnetic films with uniaxial anisotropy. *Phys. Rev. B: Condens. Mater. Phys.* **2000**, *61* (14), 9506−9512.
(62) Tao, X. D.; Wang, H. L.; Miao, B. F.; Sun, L.; You, B.; Wu, D.; Zhang, W.; Oepen, H. P.; Zhao, J. H.; Ding, H. F. Unveiling the Mechanism for the Split Hysteresis Loop in Epitaxial Co2Fe1-xMnxAl Full-Heusler Alloy Films. *Sci. Rep.* **2016**, *6*, 18615.
(63) Dumm, M.; Zölfl, M.; Moosbühler, R.; Brockmann, M.; Schmidt, T.; Bayreuther, G. Magnetism of ultrathin FeCo (001) films on GaAs(001). *J. Appl. Phys.* **2000**, *87* (5457), 5457−5459.
(64) Urone, P. P.; Hinrichs, R.; Dirks, K.; Sharma, M. *College Physics*; OpenStax College, Rice University: Houston, TX, 2013.
(65) Chen, C.-H.; Abate, A. R.; Lee, D.; Terentjev, E. M.; Weitz, D. A. Microfluidic Assembly of Magnetic Hydrogel Particles with Uniformly Anisotropic Structure. *Adv. Mater.* **2009**, *21*, 3201−3204.
(66) Nair, B. G; Nagaoka, Y.; Morimoto, H.; Yoshida, Y.; Maekawa, T.; Sakthi Kumar, D. S. Aptamer conjugated magnetic nanoparticles as nanosurgeons. *Nanotechnology* **2010**, *21*, 455102.
(67) Weeber, R.; Hermes, M.; Schmidt, A. M.; Holm, C. Polymer architecture of magnetic gels: a review. *J. Phys.: Condens. Matter* **2018**, *30*, 063002.

https://doi.org/10.1021/acs.jpcb.1c03158
J. Phys. Chem. B 2021, 125, 7900−7910